Eur Biophys J (1996) 25: 75–91

ARTICLE

Thomas Schlief · Roland Schönherr · Keiji Imoto
Stefan H. Heinemann

Pore properties of rat brain II sodium channels mutated in the selectivity filter domain

Received: 24 July 1996 / Accepted: 12 September 1996

Abstract Ion selectivity of voltage-activated sodium channels is determined by amino-acid residues in the pore regions of all four homologous repeats. The major determinants are the residues DEKA (for repeats I-IV) which form a putative ring structure in the pore; the homologous structure in Ca-channels consists of EEEE. By combining site-directed mutagenesis of a non-inactivating form of the rat brain sodium channel II with electrophysiological methods, we attempted to quantify the importance of charge, size, and side-chain position of the amino-acid residues within this ring structure on channel properties such as monovalent cation selectivity, single-channel conductance, permeation and selectivity of divalent cations, and channel block by extracellular Ca^{2+} and tetrodotoxin (TTX). In all mutant channels tested, even those with the same net charge in the ring structure as the wild type, the selectivity for Na^+ and Li^+ over K^+, Rb^+, Cs^+, and NH_4^+ was significantly reduced. The changes in charge did not correlate in a simple fashion with the single-channel conductances. Permeation of divalent ions (Ca^{2+}, Ba^{2+}, Sr^{2+}, Mg^{2+}, Mn^{2+}) was introduced by some of the mutations. The IC_{50} values for the Ca^{2+} block of Na^+ currents decreased exponentially with increasing net negative charge of the selectivity ring. The sensitivity towards channel block by TTX was reduced in all investigated mutants. Mutations in repeat IV are an exception as they caused smaller effects on all investigated channel properties compared with the other repeats.

Key words Sodium channel · Permeation · Selectivity · Oocyte expression · Mutagenesis

T. Schlief · R. Schönherr · S. H. Heinemann (✉)
Max-Planck-Gesellschaft z.F.d.W. e.V.,
AG Molekulare und zelluläre Biophysik,
Drackendorfer Strasse 1, D-07747 Jena, Germany,
(Fax: ++49 (3641) 304 542, e-mail: ite@rz.uni-jena.de)

K. Imoto
National Institute for Physiological Sciences,
Department of Information Physiology, Okazaki, 444, Japan

Introduction

Sodium channels (Na-channels) play a key role in generating action potentials in excitable cells. This task can be accomplished by a fast activation and inactivation combined with a strong ion selectivity for Na^+ with respect to K^+ and Ca^{2+}. Molecular cloning of several Na-channel α subunits has provided structural information resulting in a putative topological organization of the protein in the cell membrane as four homologous domains with each domain consisting of six transmembrane segments (for review see Catterall 1988; Heinemann and Stühmer 1995). Several studies using the approach of site-directed mutagenesis and functional assays in host cells yielded valuable information on structure-function relationships of Na-channel proteins. While voltage-dependent activation of Na-channels is at least in part associated with the positively charged S4-segments (Stühmer et al. 1989), the inactivation process is strongly influenced by the linking region between domains III and IV (Stühmer et al. 1989; West et al. 1992). Protein regions which make the actual contact with permeating ions were determined by assaying single-point mutants for their block by the specific toxins tetrodotoxin (TTX) and saxitoxin (STX). The single-point mutation in the first domain of the rat brain Na-channel II (NaRbII), E387Q, resulted in a complete loss of the blocking efficiency of TTX and STX (Noda et al. 1989). Neutralization of the neighboring charged amino-acid residue D384N not only impaired the block by TTX but also strongly reduced the single-channel conductance (Pusch et al. 1991). In a systematic study, Terlau et al. (1991) investigated the importance of the homologous sites of the remaining three domains for TTX block and ion permeation. They concluded that the outer channel mouth is in part lined by amino-acid residues forming two putative ring structures in three-dimensional space (see vertical boxes in Fig. 1A). While changes of residues in the "outer ring" have marked effects on TTX block, alterations of the residues in the "inner ring" in addition strongly affect ion permeation.

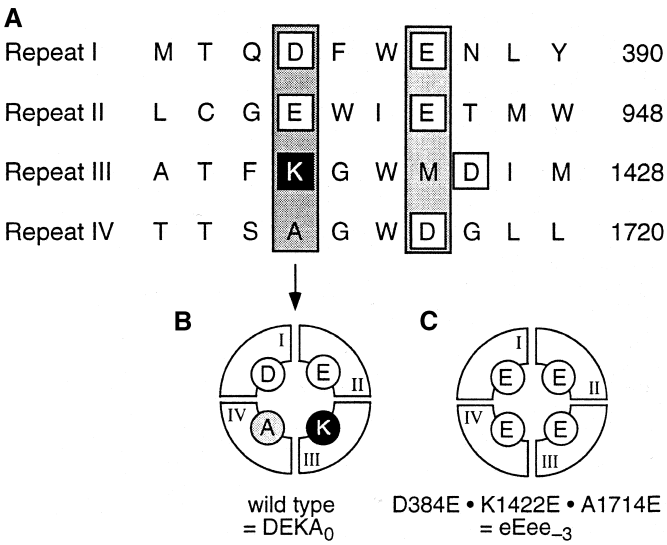

Fig. 1 **A** Alignment of amino-acid residues of the pore regions of the four homologous repeats of rat brain Na-channel II. Charged amino-acid residues are shown in squares. The numbers at the right indicate the residue number of the last amino-acid residue per row. The vertical shaded boxes indicate the residues which contribute to the putative ring structures; the left one is strongly determining the channel selectivity. **B** Schematic presentation of a top view onto the "inner ring" structure of the channel consisting of one residue per homologous repeat. The residues of interest are: D384, E942, K1422, and A1714 yielding the abbreviation "$DEKA_0$" for the wild type. **C** "$eEee_{-3}$" represents the mutant D384E·K1422E·A1714E which has the same "inner ring" structure as Ca-channels, i.e. the net charge of this structure is 3 electron charges more negative than the wild type. The mutated residues are denoted by lower-case letters

Evidently, the charged residues in the pore region of voltage-activated Na-channels are of particular importance, but non-charged residues also participate in determining channel sensitivity to TTX. F385 plays a key role for the major functional difference between the brain Na-channels (F) and the heart (C) and skeletal muscle (Y) Na-channels, by conferring the typical characteristics of channel block by TTX and divalent cations such as Cd^{2+} and Zn^{2+} (Backx et al. 1992; Heinemann et al. 1992b; Satin et al. 1992).

Although small effects on permeation and selectivity are also observed by mutating residues in the "outer ring", the major importance resides in the inner ring. When K1422 in repeat III is mutated to E, selectivity is abolished and channels become significantly permeable to Ca^{2+}; similar, but less pronounced effects are obtained by mutating A1714 in repeat IV to E (Heinemann et al. 1992a). This is not too surprising since Ca-channels have a motif consisting of four glutamates at the putative inner ring structure (Fig. 1C, EEEE). Also in Ca-channels, mutation of one of these residues to Q impairs the selectivity of the channel for Ba^{2+} over monovalent cations and reduces the block by divalent cations such as Cd^{2+} (Kim et al. 1993; Yang et al. 1993; Tang et al. 1993; Heinemann et al. 1994). Moreover, the effect of the individual residues in the four homologous repeats is not identical indicating an asymmetric organization (Kim et al. 1993; Yang et al. 1993; Heinemann et al. 1994).

In this study we concentrated on the properties of Na-channels mutated at the putative inner ring structure, focusing on ion permeation, ion selectivity, block by TTX, and block and permeation of divalent cations. We tried to address the question of the importance of charge, side-chain size and position of the amino-acid residues within the ring structure on these pore properties. Since Na-channels undergo a very rapid inactivation, we generated all pore mutants in the background of the point mutations F1489Q or I1488Q·F1489Q·M1490Q which strongly reduce inactivation (West et al. 1992) without changing the pore properties (Heinemann et al. 1994).

Materials and methods

Mutagenesis and mRNA synthesis

All mutant cDNAs were derived from the plasmid pRII-2A (Stühmer et al. 1989), encoding a wild-type rat brain Na-channel II. The plasmids are named using a four-letter code, indicating the amino-acid residues in the inner ring positions of the selectivity filter region (384, 942, 1422, 1714; wild type is DEKA). All mutations in the DEKA ring were analyzed in the background of a second mutation, introduced to prevent rapid channel inactivation. This additional mutation was either I1488Q · F1489Q · M1490Q (in DEeA and DkKA) or F1489Q (all other mutants). The introduced nucleotide changes are as follows: CAG (4465–4467) for F1489Q and CAGCAGCA (4462–4469) for I1488Q · F1489Q · M1490Q (substituted nucleotides in parentheses, numbers starting from the first ATG codon). The following replacements in inner ring positions have been described previously: D384E, D384N, E942Q, K1422E, and A1714E (Terlau et al. 1991). Additional mutations are as follows: E942K, K1422D, K1422Q, A1714D. Mutant plasmids were constructed by oligonucleotide-directed mutagenesis (Terlau et al. 1991); the mutations were confirmed by sequencing subcloned cDNA fragments. Combinations of mutations were achieved by ligation of the relevant fragments. The mutation I1488Q · F1489Q · M1490Q was introduced by using a two-step polymerase chain reaction. The first reaction was carried out with a mutagenic primer and a second primer covering a unique *Bst*EII site downstream of the mutation. The product of this reaction was then used as a primer in a second polymerase chain reaction, combined with an upstream primer covering the unique *Nsi*I site. The product of this reaction was ligated into pRII-2A, using the restriction sites *Nsi*I and *Bst*EII. The SP6 mMessage mMachine Kit (Ambion, Austin, TX, USA) was used for synthesis of capped cRNA from *Sal*I-digested plasmids.

Mutant nomenclature

Since the mutations F1489Q and I1488Q·F1489Q·M1490Q did not have effects on the pore properties tested, we refer to them as wild-type channels. All pore mutants discussed here were generated by replacing amino-acid residues of the "inner ring" structure, i.e. D384, E942, K1422, and A1714. For identification of the mutants we therefore only specify this quartet of residues in single-letter amino-acid code. Substituted residues are shown in lower case. In addition, a subscript indicates the change in net charge of the inner ring structure, Δq. As indicated in Fig. 1B, the name for the wild type is then $DEKA_0$; the triple mutant which has the same inner ring structure as Ca-channels is $eEee_{-3}$ (see Fig. 1C).

Electrophysiology

Xenopus oocytes were prepared and mRNAs were injected as described previously (Stühmer et al. 1992). Whole-cell currents were measured with a two-electrode voltage clamp (Turbo TEC 1/2, npi electronic, Tamm, Germany). Intracellular electrodes were filled with 2 M KCl and had resistances between 0.5 and 0.8 MΩ. Patch-clamp experiments were performed with an EPC-7 electronic amplifier (HEKA elektronik, Lambrecht, Germany). Pipettes for macro-patch recordings were fabricated from aluminum silicate glass and had resistances between 0.8 and 3.0 MΩ. Most single-channel recordings were performed with pipettes from thick-walled borosilicate glass with resistances between 3 and 10 MΩ. For those mutants which yielded a low expression level, single-channel recordings were also performed with aluminum glass pipettes. Data acquisition for both two-electrode clamp and patch-clamp experiments was controlled with the Pulse+PulseFit software package (HEKA elektronik) running on a Macintosh Quadra 650 computer (Apple Computer Inc., Cupertino, CA, USA). Data traces of macroscopic currents were corrected for linear leak currents and capacitive transients using a P/4 method with a leak holding potential of –110 mV. Data analysis was performed with PulseFit (HEKA elektronik) and IgorPro (WaveMetrics Inc., Lake Oswego, OR, USA). Single-channel recordings were corrected for leak and capacitive currents and single-channel voltage ramp responses were accumulated using the PulseTools software (HEKA elektronik).

All solutions with monovalent cations as the major charge carriers were made such that they contained 115 mM of the monovalent cations, i.e. approximately 108 mM of the corresponding chloride salt (e.g., NaCl) and 7 mM of the hydroxide (e.g., NaOH) for pH adjustment. In addition, these solutions contained either 1.8 mM $CaCl_2$ or alternatively 1.8 mM EGTA when Ca^{2+} had to be chelated. Solutions with divalent cations as the major charge carriers contained 75 mM of divalent cations (e.g., Ba^{2+}). The pH was buffered in all cases with 10 mM HEPES to 7.2 with the corresponding hydroxides. In the following we refer to the solutions as, e.g., Na-Ringer's: 108 NaCl, 1.8 $CaCl_2$, 10 HEPES, 7 NaOH; Na-EGTA: 108 NaCl, 1.8 EGTA, 10 HEPES, 7 NaOH; Ba75: 72 $BaCl_2$, 10 HEPES, 3 $Ba(OH)_2$.

Ca^{2+} blocks Na-channels which are mutated in the selectivity filter region to a different degree and it can contribute significantly to permeation in the mutants $DEeA_{-2}$ and $DEee_{-3}$ (Heinemann et al. 1992a; Heinemann et al. 1994). In addition, even small Ca^{2+} influx through mutated Na-channels causes a substantial activation of endogenous Ca^{2+}-activated chloride channels which are a very serious error source. In a systematic study of ion selectivity of these channels for monovalent cations, the presence of Ca^{2+} would, therefore, introduce a significant bias of the results. For this reason, selectivity of Na-channel mutants was assayed with extracellular solutions in which residual Ca^{2+} was chelated by 1.8 mM EGTA. This procedure poses a substantial problem which arises from the activation of a monovalent cationic conductance in the absence of Ca^{2+}_o (Arellano et al. 1995). These "leak" currents in EGTA solutions occur in almost all batches of oocytes and complicate the leak correction of currents flowing through the exogenously expressed voltage-dependent Na-channels. Therefore, in determining the selectivity properties, data often had to be determined in sandwiched experiments, i.e. changing the bath solution back to the control solution after each test solution in order to confirm reversibility.

Junction potentials

In cases where patch-clamp experiments are started with different solutions in the bath and in the pipette, the resulting liquid junction potential is canceled out with the pipette potential offset correction of the patch-clamp amplifier. After seal formation, this liquid junction potential is, therefore, overcompensated and has to be taken into account. We measured the junction potential shifts for all solutions used in respect to Na-EGTA according to Neher (1995). The values between –3.0 mV (Li-EGTA) and +4.9 mV (Cs-EGTA) agreed well with the theoretical predictions by Barry and Lynch (1991). Correction was done by shifting the single-channel ramps along the voltage axis accordingly.

Relative permeabilities

Reversal potentials, E_{rev}, were measured from single-channel current-voltage relationships under biionic conditions, i.e. Na-EGTA on one side and X-EGTA on the other side of the membrane (where X denotes the other tested monovalent cations). The relative permeabilities, P_X/P_{Na}, are then obtained from

$$E_{rev} = \frac{RT}{F} \ln\left(\frac{P_x}{P_{Na}}\right) \quad (1)$$

where R, T and F are the gas constant, absolute temperature, and Faraday's constant, respectively. The relative permeabilities can be also determined from two-electrode

voltage clamp recordings, without exact knowledge of the intracellular ion composition, by measuring the difference in reversal potential between the test solution (X-EGTA) and the reference solution (Na-EGTA). In the case of equal concentrations the following expression is applicable (e.g. Hille 1992):

$$\Delta E_{rev} = E_{rev}(X) - E_{rev}(Na) = \frac{RT}{F} \ln\left(\frac{P_x}{P_{Na}}\right) \quad (2)$$

Prolongation of channel open-time

NaRbII channels undergo rapid inactivation when expressed in *Xenopus* oocytes (e.g., Stühmer et al. 1989). In order to remove fast inactivation we used the mutants F1489Q or I1488Q·F1489Q·M1490Q (West et al. 1992). With these mutants long single-channel events can be measured above activation threshold which makes the compilation of single-channel ramp current-voltage relationships feasible. In addition, in particular for those channel mutants which did not express large currents, removal of inactivation allows one to distinguish the exogenously expressed channels from endogenous, inactivating Na-channels which were present in some batches of oocytes.

The open times of the Na-channel mutants at potentials below activation threshold are rather short; thus, the probability of finding an open channel in the negative part of a voltage ramp is very small. Therefore, in some experiments we used deltamethrin (DMT) which considerably slows down channel deactivation (Chinn and Narahashi 1986; Bloomquist 1996). As we could not find an influence of DMT on single-channel amplitudes in symmetrical Na-EGTA solutions, we included data obtained with DMT in our statistics for channel conductance as specified in the text and Table 1.

As to the effects of DMT on Na-channel selectivity, different reports exist. While Chinn & Narahashi (1986) found no effect on Na-channels in mouse neuroblastoma cells, Leibowitz et al. (1987) reported a change in the relative permeability P_{NH_4}/P_{Na} from 0.11 to 0.26 of Na-channels in frog skeletal muscle. We tested this permeability ratio for the wild type NaRbII channel and determined 0.24 ± 0.04 (n = 5) under control conditions and 0.20 ± 0.02 (n = 7) in the presence of 10 mM DMT. P_K/P_{Na} was tested for mutant $DEKe_{-1}$: control 0.30 ± 0.02 (n = 5); 0.28 ± 0.03 (n = 6) in 10 mM DMT. Thus, we did not find a significant influence of DMT on ion selectivity. However, as it is not safe to transfer this conclusion to all mutants tested, we tried to avoid the use of DMT whenever possible.

Results

Ion selectivity

In Fig. 2A two-electrode voltage-clamp experiments are shown for the wild type and several mutants with single amino-acid substitution in repeats I, III, or IV. Each column shows recordings from a single oocyte in the indicated test ion solutions in the absence of Ca^{2+}. The experimental protocol was to record current-voltage relationships in steps of 5 mV from a holding potential of –100 mV in solutions containing 115 NaCl in addition to 1.8 mM EGTA and 10 mM HEPES (pH 7.2). The entire bath solution was then exchanged for solutions containing instead of Na^+ the test ions Li^+, K^+, Rb^+, Cs^+, or NH_4^+. The current was measured as mean between 9 and 10 ms after the depolarization and the resulting current-voltage relationships were plotted for Na^+ (open circles), K^+ (filled circles), and Cs^+ (open squares) in Fig. 2B, indicating the alterations of ion selectivity obtained with the investigated mutations, namely changes in the reversal potential accompanied by increasing inward permeation of K^+ and Cs^+. The reversal potentials were estimated with a linear fit of a few current values around zero; the permeability ratios P_X/P_{Na} were calculated according to Eq. (2) and are summarized in Table 1 for all tested ions. Owing to large "-leak" currents developing in the absence of extracellular Ca^{2+} the entire series of monovalent cations could not be completed in all cases. Therefore, the data shown in Table 1 are based on experiments in which the various test ions were always measured with respect to Na^+.

An interesting observation in Fig. 2 is that the charge-conserving mutation $eEKA_0$ has enhanced K^+ influx compared to the wild type ($DEKA_0$); however, no Cs^+ influx could be detected. A similar result is obtained for the mutant $DEKe_{-1}$. Mutations of repeat III show marked effects on K^+ and Cs^+ permeation evidenced by a greater inward current and a positive shift of the reversal potential. Interestingly, even substitution of a neutral residue at position 1422 ($DEqA_{-1}$) is sufficient to impair selectivity of Na^+ over K^+ and Cs^+, albeit to a somewhat smaller extent (Heinemann et al. 1994).

For the same mutants as shown in Fig. 2 single-channel properties were measured in outside-out patches in the absence of Ca^{2+} on both sides of the membrane. The bath solutions contained 115 mM of the following test ions: Na^+, Li^+, K^+, Rb^+, Cs^+, and NH_4^+. In Fig. 3A only examples for Na^+, K^+, and Cs^+ are shown. Voltage ramps between +100 and –100 mV (within 200 ms) were applied and superpositions of leak-corrected single-channel current traces were plotted in Fig. 3A as a function of the ramp potential. The manually selected open-episodes of all compiled single-channel ramps (open circles) were then fitted with a double-exponential function (continuous curve) which was subsequently used to calculate the reversal potential. In addition, the fit results are shown in Fig. 3B for all tested ions on an expanded current scale. The permeability ratios were determined using Eq. (1) and are listed in Table 1. Note not only the change in permeability ratios but also the changes in single-channel conductance. While the mutations in repeat IV reduce the conductance, mutations of the site in repeat III caused, in all three cases, approximately a doubling of the single-channel conductance. Remarkable is the strong increase in permeation of NH_4^+ in these mutants. Another interesting correlation is the observed increase of P_{Li}/P_{Na} for those mutants with a small

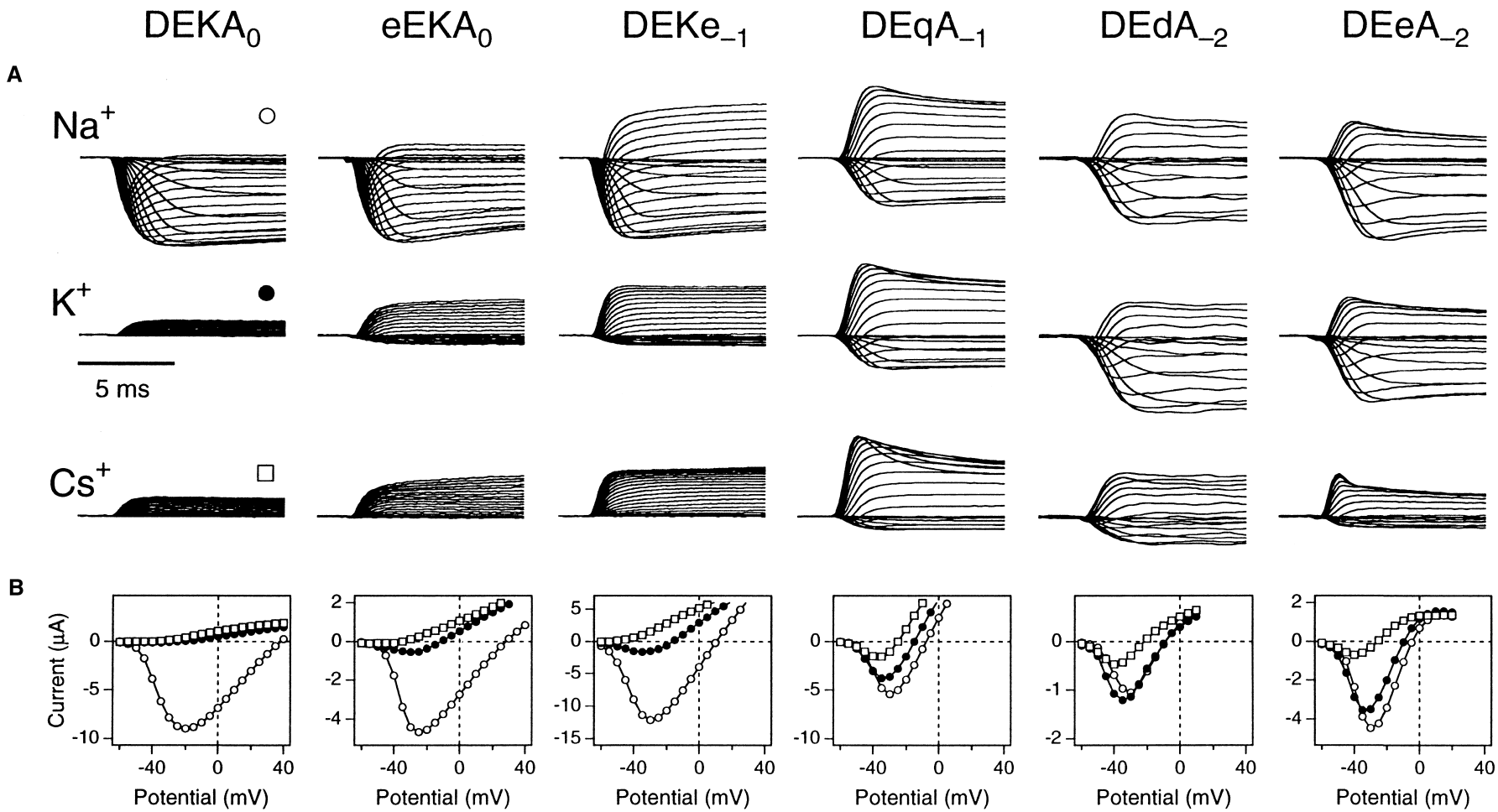

Fig. 2A, B Selectivity of Na-channels – whole-cell recordings. **A** Two-electrode voltage-clamp recordings from oocytes expressing the indicated Na-channel pore mutants. All mutants were generated in the background of the mutation F1489Q which greatly eliminates channel inactivation. Current responses were elicited by depolarizing steps starting from –60 mV in increments of 5 mV. The holding potential was –100 mV. Extracellular bath solutions were in addition to 1.8 mM EGTA and 10 mM HEPES, 108 mM NaCl, KCl, or CsCl pH-adjusted with the corresponding hydroxides yielding a total concentration of the monovalent cations of 115 mM (Na-EGTA, K-EGTA, Cs-EGTA) as indicated at the left. Each column shows recordings from one oocyte. **B** Mean currents obtained between 9 and 10 ms were plotted as a function of the test potential (Na^+: *open circles*; K^+: *filled circles*; Cs^+: *open squares*). The symbols were connected with straight lines. Average values for the determined permeability ratios are listed in Table 1. Filter frequency: 1 kHz

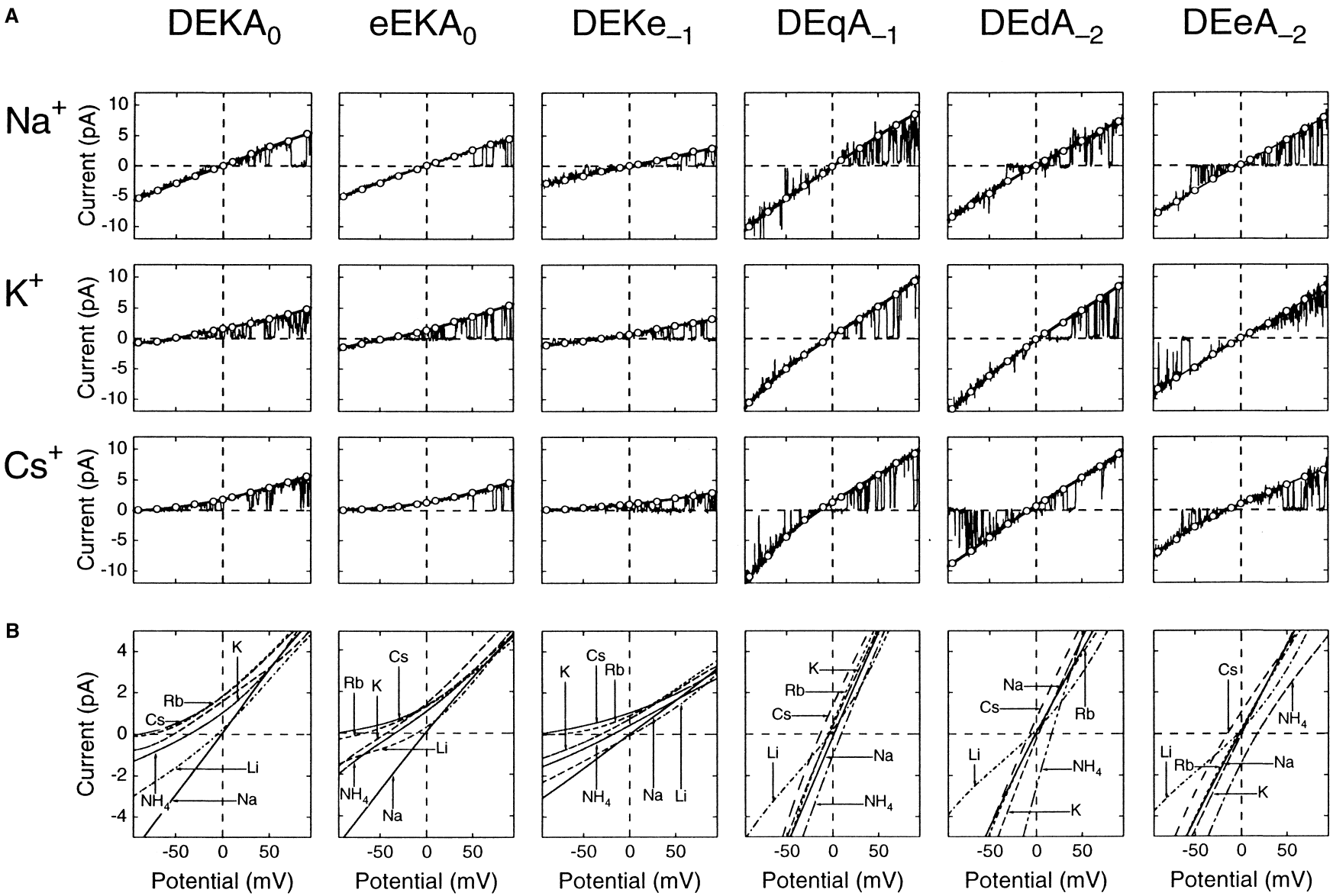

Fig. 3 A, B Single-channel voltage-ramp responses. **A** Single-channel current events in response to voltage ramps between +100 and –100 mV from a holding potential of –80 mV (200 ms) are shown for the indicated Na-channel pore mutants in the background of the inactivation mutant F1489Q. As it was a rare event of finding a single channel in the open state throughout the ramp period, some current traces were compiled from several ramp sweeps. The recordings were obtained in the outside-out patch-clamp configuration with Na-EGTA in the pipette solution. The bath medium contained Na-EGTA, K-EGTA, or Cs-EGTA, as indicated at the left of the figure. The single-channel current-voltage relationships were idealized by eye. **B** The resulting idealized functions were plotted in the lower panels for the three test ions Na^+, K^+, and Cs^+. In addition, data for Li^+, Rb^+, and NH_4^+ are included. The resulting permeability ratios are listed in Table 1. Filter frequency: 2 kHz

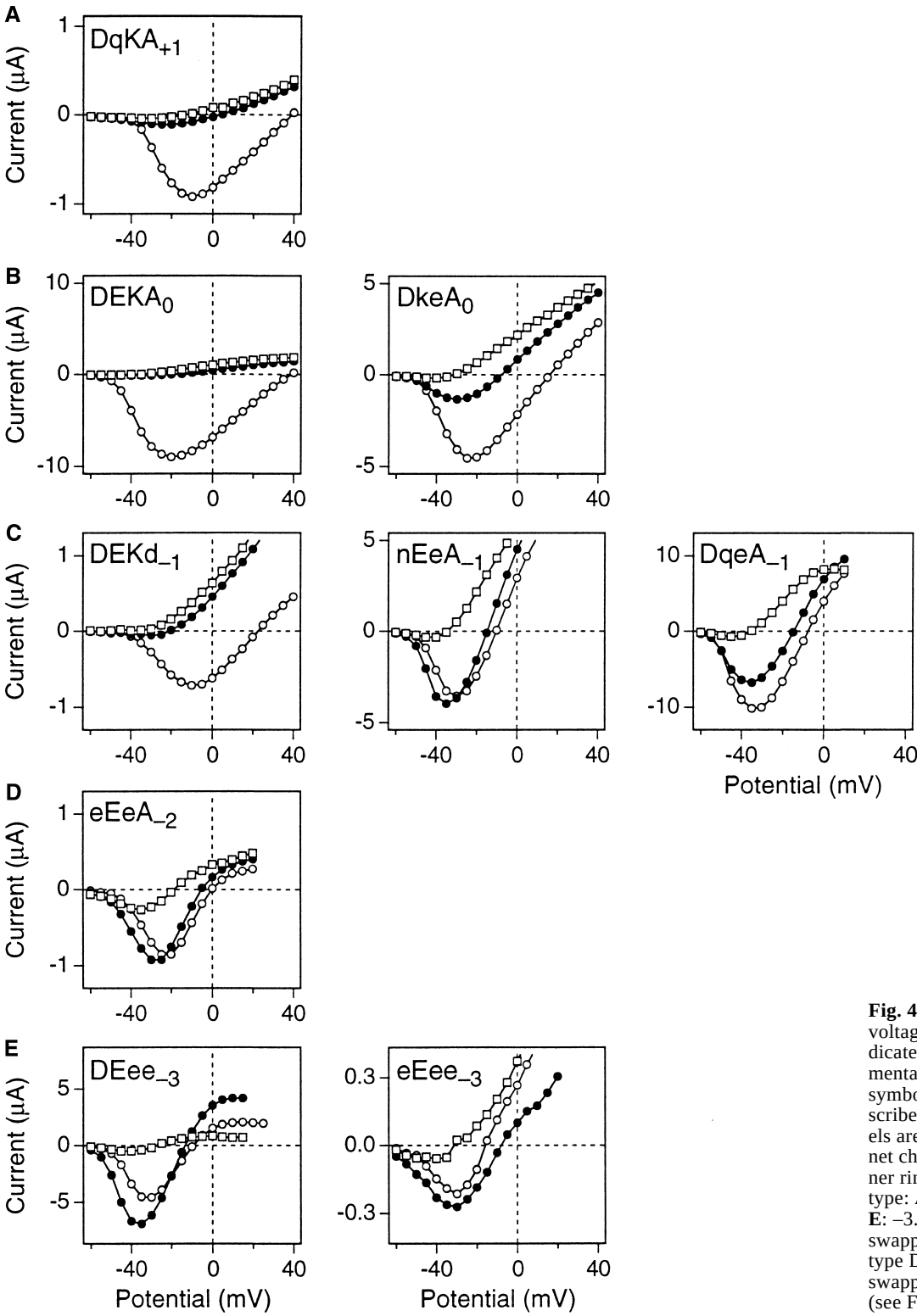

Fig. 4A–E Whole-cell current-voltage relationships for the indicated mutants. The experimental protocol and the use of symbols was the same as described in Fig. 2. The data panels are grouped according to the net change in charge of the inner ring relative to the wild type: **A**: +1, **B**: 0, **C**: –1, **D**: –2, **E**: –3. Note that $DkeA_0$ is a swapping mutant of the wild type $DEKA_0$, and $DqeA_{-1}$ is the swapping mutant of $DEqA_{-1}$ (see Fig. 2)

reduction of the single-channel conductance ($DkeA_0$, $DEKe_{-1}$, and $DEKd_{-1}$).

There are no charge altering mutants of repeats I and II shown in these panels because they have a very small conductance which is not suited for single-channel recordings (Terlau et al. 1991).

In Fig. 4 further examples for current-voltage plots in Na-, K-, and Cs-EGTA are shown, sorted according to the net negative charge in the inner ring structure. Here we also considered changes in repeats I and II which were in part compensated by mutations in other repeats. It is interesting to note that the wild type apparently has the maximal

Table 1 Single-channel conductance and permeability ratios. For the mutants listed in the first column the range of the determined single-channel conductances (γ) in symmetrical Ca^{2+}-free 115 mM NaCl solutions is displayed in the second column. *n* specifies the number of single-channel patches, *n** the number of patches in the presence of 10 μM deltamethrin. P_X/P_{Na} for the indicated test ions is shown in the remaining columns. The first row per mutant specifies the values determined from whole-oocyte experiments (see Eq. (2)), the second row contains estimates based on single-channel ramp recordings (see Eq. (1)). The numbers in parentheses indicate the number of independent experiments.

Mutant	γ(pS) (n; n*)	P_X/P_{Na} (whole oocytes & single-channel ramp recordings)				
		Li^+	K^+	Rb^+	Cs^+	NH_4^+
$DkKA_{+2}$	«1	(no ionic currents measurable)				
$DqKA_{+1}$	«1	0.98 ± 0.05 (3)	0.17 ± 0.03 (5)	0.12 ± 0.03 (3)	0.11 ± 0.03 (3)	0.28 ± 0.02 (4)
$DEKA_0$	55–62 (12; 3)	0.96 ± 0.14 (4) 0.79	0.10 ± 0.03 (8) 0.13	< 0.05 (4) < 0.05	< 0.05 (5) < 0.03	0.20 ± 0.03 (3) 0.24
$DkeA_0$	7–13 (6; 2)	1.59 ± 0.06 (3) n.d.	0.37 ± 0.03 (3) n.d.	0.25 ± 0.01 (3) n.d.	0.14 ± 0.02 (3) n.d.	2.45 ± 0.14 (3) n.d.
$eEKA_0$	45–55 (4; 0)	0.90 ± 0.06 (3) 0.67	0.22 ± 0.03 (4) 0.18	< 0.10 (4) 0.07	< 0.10 (3) < 0.03	0.54 ± 0.13 (3) 0.27
$DEKe_{-1}$	28–39 (4; 0)	1.54 ± 0.27 (4) 1.13	0.27 ± 0.04 (8) 0.29	0.13 ± 0.04 (4) 0.05	< 0.05 (6) < 0.03	0.56 ± 0.08 (5) 0.49
$DEKd_{-1}$	17–24 (3; 2)	1.74 ± 0.39 (5) n.d.	0.23 ± 0.05 (5) n.d.	0.11 ± 0.11 (5) n.d.	0.08 ± 0.08 (5) n.d.	0.53 ± 0.20 (5) n.d.
$DEqA_{-1}$	90–110 (7; 4)	1.10 ± 0.16 (4) 0.89	0.76 ± 0.06 (6) 0.86	0.66 ± 0.09 (5) 0.82	0.50 ± 0.05 (6) 0.59	1.51 ± 0.59 (5) 1.45
$DqeA_{-1}$	46–53 (4; 1)	1.20 ± 0.05 (4) n.d.	0.74 ± 0.02 (4) n.d.	0.53 ± 0.02 (4) n.d.	0.32 ± 0.01 (3) n.d.	1.69 ± 0.02 (4) n.d.
$nEeA_{-1}$	54–65 (3; 2)	1.06 ± 0.18 (4) n.d.	0.87 ± 0.02 (3) n.d.	0.65 ± 0.01 (3) n.d.	0.42 ± 0.06 (3) n.d.	1.80 ± 0.12 (5) n.d.
$DEeA_{-2}$	72–85 (8; 1)	0.97 ± 0.01 (3) 0.88	0.83 ± 0.03 (4) 1.03	0.66 ± 0.02 (3) 0.89	0.42 ± 0.02 (3) 0.56	1.66 ± 0.09 (3) 2.02
$DEdA_{-2}$	88–100 (7; 2)	1.01 ± 0.03 (3) 0.85	0.92 ± 0.02 (3) 1.1	0.83 ± 0.05 (3) 0.97	0.61 ± 0.03 (3) 0.74	1.55 ± 0.34 (3) 1.92
$eEeA_{-2}$	90–100 (4; 3)	0.96 ± 0.26 (7) n.d.	0.84 ± 0.07 (8) n.d.	0.69 ± 0.01 (4) n.d.	0.52 ± 0.07 (6) n.d.	1.48 ± 0.25 (5) n.d.
$DEee_{-3}$	72–78 (4; 4)	0.99 ± 0.03 (4) n.d.	0.95 ± 0.05 (4) n.d.	0.83 ± 0.04 (4) n.d.	0.65 ± 0.07 (3) n.d.	1.37 ± 0.12 (3) n.d.
$eEee_{-3}$	70–90 (3; 2)	1.04 ± 0.16 (5) n.d.	1.03 ± 0.08 (4) n.d.	0.94 ± 0.14 (4) n.d.	0.48 ± 0.11 (3) n.d.	1.14 ± 0.24 (4) n.d.

selectivity for Na^+ over K^+; in the residue-swapping mutant $DkeA_0$ and even in the mutant $DqKA_{+1}$ with a more positive ring structure, P_K/P_{Na} is clearly greater than for the wild type (see also Table 1).

Single-channel conductance

The single-channel currents of the mutants were determined in outside-out or inside-out patches with symmetrical Na-EGTA solutions in order to avoid Ca^{2+} block. For most mutants the slope conductance was determined from single-channel ramp recordings (see Fig. 3A, first row). Owing to the small chance of channel opening at negative potentials this approach failed for those mutants which did not express well. Therefore, some of the conductance determinations shown in Table 1 were complemented by chord conductances based on measurements of single-channel currents at –100 mV and +100 mV in the presence of deltamethrin which considerably slows down channel deactivation (Chinn and Narahashi 1986; Bloomquist 1996). In Table 1 the number of experiments in which deltamethrin was used is specified as the second number in parentheses (n*). While mutants with a positive inner ring structure had very low conductances, net charge reduction in repeat III resulted in conductances as high as about 100 pS, i.e. almost twice the value of the wild type. As will be shown later (see e.g., Fig. 9), measurements in Na-Ringer's as extracellular solution yield quite different estimates.

Permeation of divalent cations

As noted for mutant $DEeA_{-2}$ previously (Heinemann et al. 1992a), Ba^{2+} can readily permeate through this mutated Na-channel when the lysine residue at position 1422 is replaced by a glutamate. For the mutants of the inner ring structure we quantified the relative permeability of Ba^{2+} versus Na^+ by measuring the reversal potential in two-electrode voltage-clamp experiments both in extracellular Ba75 and in Na-EGTA. In Fig. 5A four examples of such current-voltage plots are shown for mutants with changes in the net charge between 0 and –3. The wild type is not shown as we did not detect any sign of Ba^{2+} permeation; the criterion for the detection of Ba^{2+} permeation was the appearance of a negative-slope region in the current-voltage plots. The indicated reversal potentials for these experiments clearly show the trend of a negative shift of the reversal potential for Na-EGTA concomitant with a positive shift of the reversal potential for Ba^{2+} when the net charge is made more negative. Note that the activation is shifted to more positive potentials in the presence of 75 mM $BaCl_2$ which results in only very small inward currents in mutants with a low reversal potential (e.g., $DkeA_0$, $DEqA_{-1}$). In Fig. 5B the mean reversal potentials in Ba75 are plotted for various mutants versus Δq. The continuous line is a linear fit indicating the strong correlation of E_{rev}(Ba) and Δq.

Permeation of other divalent cations was determined by replacing 75 mM $BaCl_2$ by $MgCl_2$, $MnCl_2$, $CaCl_2$, or $SrCl_2$ and by measuring the maximum inward current obtained in two-electrode voltage-clamp experiments. Such a determination of divalent permeation is complicated by three major obstacles. (1) As already mentioned for the measurements of Ba^{2+} reversal potentials, divalent cations shift the voltage dependence of channel activation to positive potentials yielding only small open probabilities below the reversal potentials of the divalent cations. (2) Most mutants do not conduct divalent cations very well. (3) In particular the influx of Ca^{2+} and Sr^{2+} activates huge Ca^{2+}-dependent chloride currents which severely mask the actual Ca^{2+} or Sr^{2+} influx. As an example it is shown in Fig. 6 how a substitution of K1422 in repeat III by an aspartate ($DEdA_{-2}$) results in permeation of the divalent cations Mn^{2+} and Mg^{2+}; the influx of Ca^{2+} and Sr^{2+} activates Cl-currents which greatly overwrite the small currents carried by the divalent cations. Because of the experimental obstacles mentioned above, we only attempted to make a qualitative classification of the mutants with respect to the permeation of divalent cations. We distinguished between mutants which permit clearly resolvable inward currents (++) like those for mutant $DEdA_{-2}$ in Ba^{2+} and Mg^{2+} (Fig. 6), those with barely resolvable currents (+) (Mn^{2+}, Ca^{2+}, Sr^{2+} in Fig. 6), those which only show the activation of chloride channels upon opening of the Na-channels ("Cl-currents"), and mutants where no sign of inward current or chloride current could be detected (–). Such a classification of the investigated mutants is shown for Ca^{2+} permeation in Table 2. The permeation of both, Ba^{2+} and Sr^{2+} was similar to that of Ca^{2+}. Exceptions were

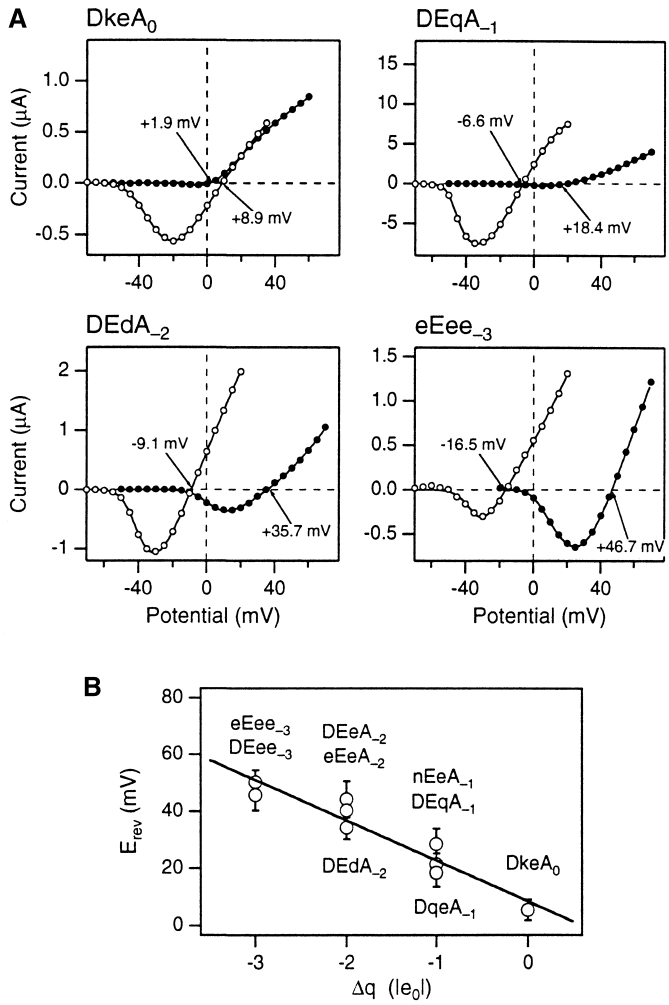

Fig. 5 **A** Current-voltage relationships of mutants $DkeA_0$, $DEqA_{-1}$, $DEdA_{-2}$, and $eEee_{-3}$ determined in two-electrode voltage-clamp experiments from one oocyte each. The extracellular medium was Na-EGTA (open symbols) or Ba75 (filled symbols). The estimated reversal potentials are indicated by the arrows. **B** Ba^{2+} reversal potentials determined from experiments as shown in **A** plotted versus the change in the net charge of the inner ring relative to the wild type for the indicated mutants. The error bars indicate S.D. values based on 3–7 experiments. The continuous line is the result of a linear fit with a slope of –14 mV/e_0 and an intersect of 8.5 mV

the mutants $DEqA_{-1}$ ($Ca^{2+} > Ba^{2+}$, Sr^{2+}) and $DEdA_{-2}$ ($Ba^{2+} > Ca^{2+}$, Sr^{2+}) (n=3–12). In addition, no chloride currents could be detected for mutant $DEKd_{-1}$ in the presence of external Sr^{2+}.

Small Mg^{2+} inward currents were also observed for mutants $DEqA_{-1}$ (n=5) and $eEeA_{-2}$ (n=4); Mn^{2+} currents were detectable in mutants $DEqA_{-1}$ (n=5), $DEeA_{-2}$ (n=5), and $eEeA_{-2}$ (n=4). It is interesting to note that no permeation of Mg^{2+} or Mn^{2+} could be detected in mutants with Δq=–3. In addition, substitution of glutamate by aspartate in repeat III yielded a strong increase in Mg^{2+} permeation ($DEeA_{-2} \rightarrow DEdA_{-2}$) while a similar substitution in repeat I caused a reduction in Mg^{2+} permeation ($eEeA_{-2} \rightarrow DEdA_{-2}$).

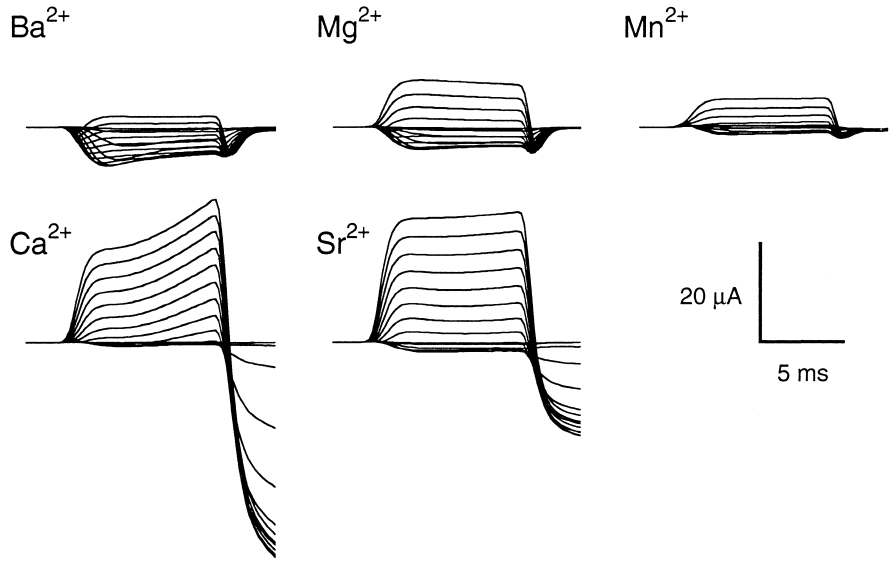

Fig. 6 Permeation of divalent cations through the mutant channel DEdA$_{-2}$. Whole-cell currents from one oocyte in response to step-depolarizations of 10 ms duration from –20 to +55 mV in steps of 5 mV from a holding potential of –80 mV. The bath solutions contained 10 mM HEPES and 75 mM chloride salt of the indicated divalent cations. Note the inward current carried by Ba^{2+}, Mg^{2+}, and Mn^{2+}. Current traces obtained in Ca^{2+} and Sr^{2+} solutions are strongly affected by Ca^{2+}-activated chloride currents which can also be activated by Sr^{2+}

Table 2 Ca^{2+} permeation and inhibition of Na^+ currents by Ca_o^{2+} and TTX. A qualitative estimate of the Ca^{2+} permeation, and the half-maximal block concentrations of Ca_o^{2+} and TTX are listed for the indicated mutants. The permeation of Ca^{2+} was assayed with Ca75 solutions in the bath; it was classified in four groups: "++": readily observable inward currents, "+": small inward currents, "Cl-current": the influx of Ca^{2+} or Sr^{2+} could only be detected indirectly by the activation of chloride channels; "–": no Ca^{2+} permeation detected. Ca_o^{2+} block was measured in external solutions based on 115 mM NaCl. TTX was added to 115 mM NaCl, 2.5 mM KCl, 1.8 mM $CaCl_2$ (pH 7.2). The numbers in parentheses indicate the number of independent experiments.

Mutant	Ca^{2+} permeation (qualitatively)	IC_{50} (Ca_o^{2+}) (µM)	IC_{50} (TTX) (nM)
$DkKA_{+2}$	– (3)	(no Na^+ currents measurable)	
$DqKA_{+1}$	– (3)	3,560 ± 2,180 (3)	> 10,000 (5)
$DEKA_0$	– (3)	8,400 ± 1,000 (4)	18 ± 4 (6)
$DkeA_0$	+ (6)	4,830 ± 810 (3)	> 10,000 (5)
$eEKA_0$	– (3)	10,600 ± 2,650 (3)	55 ± 39 (4)
$DEKe_{-1}$	Cl-currents (4)	119 ± 18 (3)	990 ± 220 (7)
$DEKd_{-1}$	Cl-currents (6)	378 ± 205 (5)	123 ± 61 (3)
$DEqA_{-1}$	++ (5)	269 ± 91 (6)	> 10,000 (3)
$DqeA_{-1}$	++ (4)	198 ± 97 (2)	> 10,000 (3)
$nEeA_{-1}$	++ (5)	335 ± 89 (3)	> 10,000 (3)
$DEeA_{-2}$	++ (5)	72 ± 12 (8)	> 10,000 (4)
$DEdA_{-2}$	+ (5)	45 ± 25 (4)	> 10,000 (4)
$eEeA_{-2}$	++ (5)	33 ± 8 (4)	> 10,000 (3)
$DEee_{-3}$	++ (4)	7.0 ± 3.2 (10)	> 10,000 (3)
$eEee_{-3}$	++ (5)	2.1 ± 0.9 (8)	> 10,000 (4)

Channel block by Ca_o^{2+} and TTX

The investigated mutants differ strongly in their block by extracellular divalent cations which complicates a systematic investigation. On the one hand, it would be nice to use divalent cations which also strongly block Ca-channels such as Cd^{2+} or Zn^{2+}. These ions are quite useful for determining block concentrations as low as approximately 10 µM. Solutions with lower concentrations of these blockers cannot be made without buffering the residual Ca^{2+}; since Ca^{2+} chelators also have high affinities for other divalent cations there is no straightforward way of generating a reasonable concentration series. On the other hand, the use of Ca^{2+} as blocking divalent cation has the disadvantage of giving rise to Ca^{2+}-activated chloride currents if Ca^{2+} contributes to ion permeation as is the case for most mutants investigated (see e.g., Fig. 6). Despite these technical problems, we attempted to determine the sensitivity of the mutants for extracellular Ca^{2+} by measuring maximum sodium inward current under two-electrode voltage-clamp control in solutions where 115 mM NaCl was gradually replaced by $CaCl_2$. This experimental protocol gives quite accurate results for IC_{50} values below 1 mM. At higher Ca^{2+} concentrations (as needed for the wild type, for example), the shift in the activation potential due to a considerable change in surface charge and a concomitant reduction of the extracellular Na^+ concentration results in a systematic underestimation of the block concentration.

In Fig. 7A two Ca^{2+} block experiments for the wild type ($DEKA_0$) and mutant $eEee_{-3}$, i.e. the mutant whose inner ring structure is identical to those of Ca-channels, are compared. While the wild type is only blocked by quite high $[Ca^{2+}]_o$ (8.4 ± 1.0 mM, n=4), the mutant is half-maximally blocked by 2.1 ± 0.9 µM (n=8); the inward current, carried by Ca^{2+}, increases again above 100 mM Ca^{2+}_o. A similar phenomenon, albeit occurring at higher $[Ca^{2+}]_o$, was previously observed for the inactivating mutant $DEeA_{-2}$ (Heinemann et al. 1992a). In this respect the Na-channel mutant $eEee_{-3}$ shows properties very similar to Ca-channels; sodium currents through the Ca-channel BI from rabbit brain, for example, are half-maximally blocked by 0.6 µM Ca_o^{2+} (Heinemann et al. 1994). A greater difference

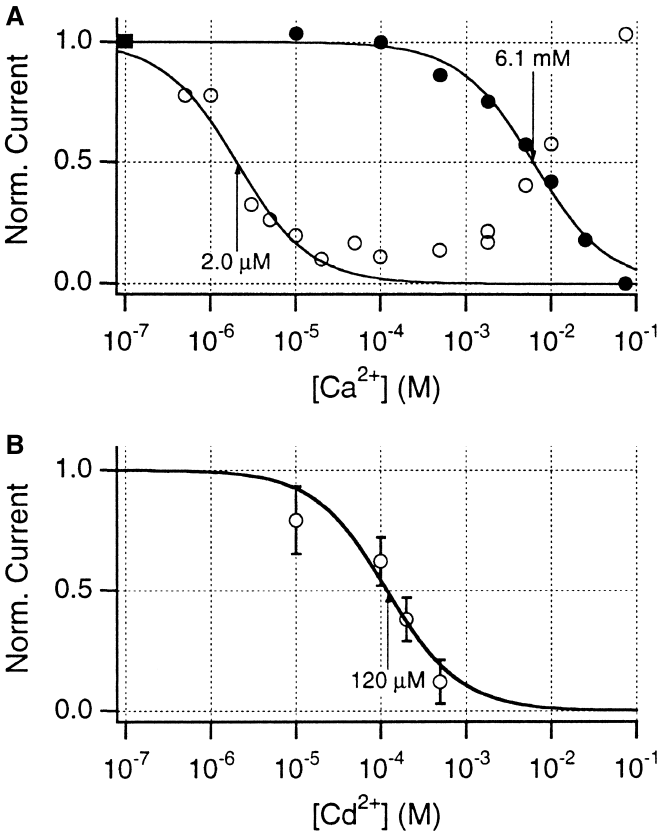

Fig. 7A, b Block and permeation of divalent cations. **A** Maximum inward current of whole-cell current-voltage relationships where 115 mM extracellular Na^+ was gradually replaced by Ca^{2+}. The current was normalized to the values obtained in the absence of Ca^{2+}. The wild type (*filled circles*) is only blocked at high $[Ca^{2+}]_o$ and shows only marginal Ca^{2+} permeability. The mutant $eEee_{-3}$ (*open circles*), however, is blocked at low $[Ca^{2+}]_o$; at higher $[Ca^{2+}]_o$ the current increases again as Ca^{2+} itself becomes the dominant charge carrier. The continuous curves correspond to dose-response plots with a Hill coefficient of 1.0 and $IC_{50}(Ca_o^{2+})$ values of 6.1 mM (wild type) and 2.0 µM ($eEee_{-3}$). Mean $IC_{50}(Ca_o^{2+})$ values of all mutants are listed in Table 2. B Block of inward Ba^{2+} currents through mutant $eEee_{-3}$ by extracellular Cd^{2+}. The indicated fit resulted in an $IC_{50}(Cd_o^{2+})$ value of 120 µM. The error bars indicate S.D. values based on 3–9 experiments

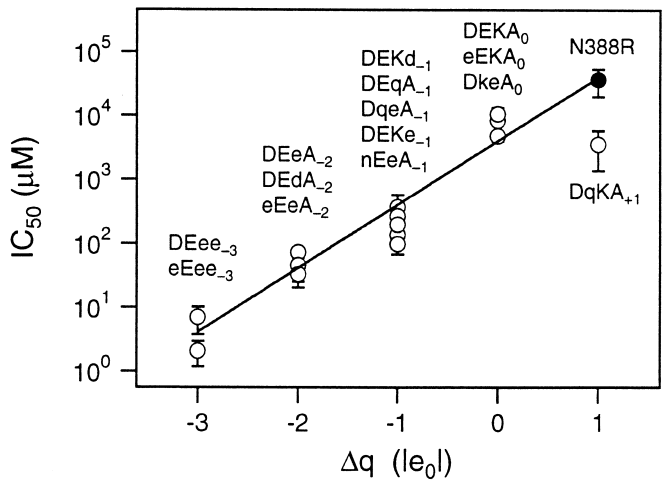

Fig. 8 Calcium block as a function of the change in net charge of the inner ring relative to the wild type. For the indicated mutants $[Ca^{2+}]_o$ necessary to block 50% of sodium inward current is plotted as a function of the net change in charge of the inner ring. Data points are given as mean±S.D. for 3–7 independent experiments. For a comparison, mutant N388R which is located downstream of the inner ring position in repeat I is shown as filled circle. The continuous line indicates an exponential function $a \cdot \exp(b \cdot \Delta q)$, with a = 4.0 mM and b = 2.29, which is the result of a least-squares fit to the data between Δq of –3 to 0

exists for the Cd^{2+} block of Ba^{2+} inward currents; while the Ca-channel BI is blocked by 1.1 µM Cd^{2+} (Heinemann et al. 1994), the $IC_{50}(Cd_o^{2+})$ value for the Na-channel mutant $eEee_{-3}$ is 120 µM (Fig. 7B).

In Fig. 8 the mean $IC_{50}(Ca_o^{2+})$ values for all mutants are plotted versus Δq. The continuous line describes an exponential function indicating a strong correlation between the block concentration and charge in the inner ring (see legend to Fig. 8); only mutant $DqKA_{+1}$ deviates from this correlation. The filled symbol represents data obtained from mutant N388R (Heinemann et al. 1992b) which is located four residues downstream of the inner ring in repeat I. The values for Ca_o^{2+} block concentrations are also listed in Table 2.

TTX block of sodium inward current was measured in two-electrode voltage-clamp experiments in the presence of 1.8 mM $CaCl_2$ in the bath solution. The determined IC_{50}(TTX) values are listed in Table 2. Most mutations have a very strong impact on TTX block. Interestingly, mutations of repeat IV cause a reduction of TTX affinity to a smaller extent. In repeats I and IV it could be demonstrated that the IC_{50}(TTX) is greater with a glutamate residue in the inner ring position compared with an aspartate. The importance of the position of the residues within the ring structure is shown by the swapping mutant $DkeA_0$ which is insensitive to TTX.

Voltage dependence of Ca_o^{2+} block

So far the sensitivity of the mutants for extracellular Ca^{2+} was determined in two-electrode voltage-clamp experiments by measuring the maximum inward sodium current. Owing to the Ca^{2+}-induced shift in the activation potential and the expected voltage dependence of Ca_o^{2+} block this approach can only give rough estimates. Therefore, we performed several outside-out patch-clamp experiments with symmetrical Na^+ on either side of the membrane, 1.8 mM EGTA on the inside, and 1.8 mM Ca^{2+} on the outside. Superpositions of single-channel ramp recordings are shown in Fig. 9 for the indicated mutants. For a comparison, the idealized single-channel current-voltage relationships obtained in symmetrical Ca^{2+}-free solutions (see Fig. 3) are superimposed. The voltage dependence of Ca_o^{2+}

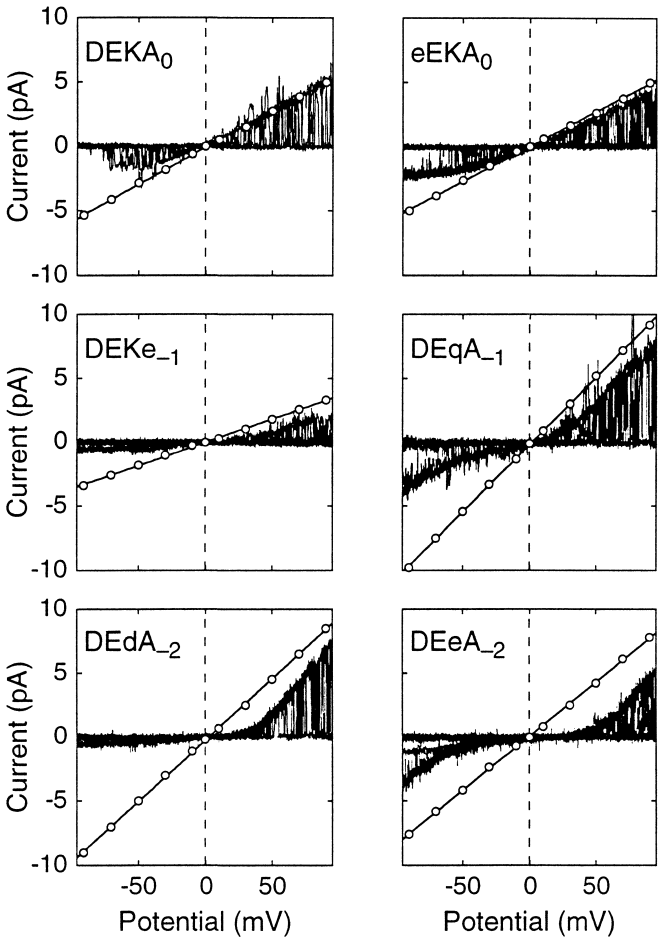

Fig. 9 Superpositions of several outside-out single-channel recordings in response to voltage ramps for the indicated mutants. The pipette solution was Na-EGTA, while the bath contained Na-Ringer, i.e. 115 mM NaCl and 1.8 mM $CaCl_2$. Filter frequency: 2 kHz. For a comparison, idealized current-voltage relationships determined in symmetrical Na-EGTA (see Fig. 3, first row) were superimposed. The current deflections at negative potentials of some data sweeps recorded for mutants $DEqA_{-1}$ and $DEeA_{-2}$ presumably are the result of Ca^{2+}-activated chloride currents

block is clearly apparent. For those mutants which significantly conduct Ca^{2+}, a problem arises at negative potentials where, even in excised membrane patches, the Ca^{2+} influx activates chloride channels causing a downward deflection of the current-voltage relationship (e. g. $DEeA_{-2}$).

Discussion

The effects of the replacement of one or more of the four different amino-acid residues in the DEKA ring of the rat brain sodium channel II, i.e. D384-E942-K1422-A1714, were investigated. The single-channel conductance, the selectivity for monovalent as well as divalent cations, and the block of the channel by TTX and divalent cations have been determined. In particular for the determination of monovalent cation selectivity and single-channel conductance we attempted to isolate these mechanisms from those of Ca^{2+} permeation and channel block by Ca_o^{2+} which becomes very significant in channel mutants with negatively charged inner ring structures. Therefore, we emphasized recordings in Ca^{2+}-free solutions despite the technical complications involved.

As wild-type Na-channels undergo rapid inactivation upon depolarization, we took advantage of channel mutations which substantially slowed inactivation: this enabled us to measure reversal potentials much more accurately than is possible for quickly inactivating channels.

One focus of interest was to elucidate the structural and functional differences as well as the similarities between Na- and Ca-channels which possess four identical amino-acid residues at the corresponding sites of the inner ring structure (EEEE). The net charge of the inner ring structure of the Na-channel is –1, whereas the Ca-channel has a net charge of –4. Therefore, we constructed several mutants in order to explore the contribution and the specificity of the charge and the structure of the amino acids at the four positions. When discussing the specificity of the four residues in the Na-channel in respect to Ca-channels one has to keep in mind that Na-channels exhibit a greater diversity among their four domains with regard to those residues adjacent to the DEKA or EEEE ring, respectively (e.g., Heinemann et al. 1992a, 1994).

Selectivity for monovalent cations

Unique to our study of the selectivity for monovalent cations are the ionic conditions because the solutions did not contain free Ca^{2+}. This has the advantage that no block or permeation of Ca^{2+} interferes with the measurement of monovalent permeation. This is especially important for those mutants which show a stronger binding of Ca^{2+} of several orders of magnitude compared to the wild type (and even exhibit divalent ion permeation at higher concentrations). The disadvantages of this procedure consist of a greater “leak” current (Arellano et al. 1995) in the two-electrode voltage-clamp measurements and the difficulty of getting high seal resistances in the patch-clamp configuration.

All investigated mutants show increased relative permeabilities P_X/P_{Na} (Table 1). The values determined from reversal potential measurements in the two-electrode voltage clamp (Fig. 2) and patch clamp (Fig. 3) are very similar. This suggests that the various problems introduced by using Ca^{2+}-free solutions are not too severe. Apparently, all four residues in the DEKA ring of NaRbII contribute to the ion selection process. Up to now this was only shown for the residues K1422 and A1714 (Heinemann et al. 1992a). The contribution to ion selectivity is not the same for the four residues although it is not possible to postulate an exact ranking for the different importance of the four different residues. However, it is evident that among the four domains position 1422 has the greatest influence

on selectivity. This is exemplified by comparing the mutant $DEqA_{-1}$ on the one hand with the mutant $DEKe_{-1}$ (or $DEKd_{-1}$) on the other hand. These mutants have equal net charge but the channel with the mutation at position 1422 has lost its selectivity to a much greater extent. This result implies at the same time that the net charge of the selectivity filter domain is not the only determinant of ion selectivity. If this were the case, mutant $DqKA_{+1}$ should not exhibit reduced relative permeabilities either. Further support for the charge not being the only determinant comes from a study of Favre et al. (1996) who found in the mutant $DErA_0$ an almost complete loss of selectivity for Na^+ over K^+.

Comparing the effects of substituting glutamates for aspartates (or *vice versa*) gives an indication of how important this small change in side-chain length (one CH_2-group) is for the channel properties. As can be seen from Table 1, these substitutions do not have a strong influence on the selectivity among monovalent cations.

In Fig. 3 it is demonstrated that not only the relative permeabilites (as judged from the reversal potential) are affected by the mutations; also the relative conductances γ_X/γ_{Na} (as may be determined from comparing the single-channel current amplitudes for the different ions at the same voltages) are changed. These results indicate that energy profiles for the permeating monovalent cations are affected by the mutations in a complex way. However, although the relative permeabilities P_X/P_{Na} are increased in all mutants, the Eisenman sequences of these channels are almost unaltered, i.e. they follow the sequences X or XI (see e.g. Hille 1992). Therefore, according to the Eisenman formalism, the binding site remains a strong one after mutation. The reduced selectivity in the mutants could, therefore, indicate that the bigger alkali ions come closer to the binding sites than in the wild type.

Recent studies employing the scanning cysteine mutation method (Kürz et al. 1995) indicate a contribution to the ion selection process of residues outside the selectivity filter. After substitution of cysteines for these residues (located between the inner and the outer ring, or at the outer ring), a reduction in selectivity was observed (Chiamvimonvat et al. 1996a, b, Pérez-García et al. 1996, Tomaselli et al. 1995, Tsushima et al. 1996). However, some of the residues have been replaced by amino-acid residues other than cysteine, resulting in no change in selectivity (Heinemann et al. 1992a). Consequently, a final statement can not be made at the moment about whether the introduced cysteines cause the reduction in selectivity because of their specific nature (perhaps by forming disulfide bonds with endogenous cysteines) or whether the residues at the positions outside the DEKA ring really contribute directly to the ion selection.

Single-channel amplitude

The single-channel conductances are affected by mutations at all four positions in the DEKA ring (Table 1). As holds for the selectivity discussed above, the net charge in this structure is not the only determinant of γ (see e.g. the swapping mutants $DEKA_0/DkeA_0$ and $DEqA_{-1}/DqeA_{-1}$). However, an interesting statement can be made if one compares the changes as a function of charge when only mutations in one domain are considered. In this pairwise comparison the other residues in the ring structure remain the same (no matter if they are native or mutated). As shown in Fig. 10A, mutations which leave the net charge constant have no significant influence on γ. However, mutations which change the net charge of the ring have a strong effect: the more positive the net charge, the smaller is γ. The opposite is true for mutations at position 1714 in domain IV. This finding is a clear indication for the functional asymmetry of the residues which constitute the selectivity filter. Concerning the positions in domains I-III it is easy to imagine that the enhanced ion flux with more negative charges in the inner ring is a consequence of the enhanced Coulomb interactions.

The special role of position 1714 may be explained in different ways. A simple steric hindrance via the longer side chains of aspartate or glutamate in comparison to the native alanine could be responsible for the reduction of γ. However, aspartate has a shorter side chain than glutamate, but $DEKd_{-1}$ has a smaller γ than $DEKe_{-1}$. Additionally, position 1714 may not be 'in-line' with the other residues in the filter region either pointing more to the external side or to the internal. The latter possibility was also suggested by Cd^{2+}-blocking experiments with cysteine mutants (Pérez-García et al. 1996; Chiamvimonvat et al. 1996b) and distance estimates between presumably adjacent pore-lining residues (Bénitah et al. 1996). In addition, the ability of the amino-acid residues to coordinate water molecules around the permeating Na^+ may be hindered by introducing a carboxyl group at position 1714. Although the molecular details for the contribution of repeat IV to ion permeation remain elusive, it is quite clear that it deviates from the other repeats.

Channel block and Coulomb interaction

The block and permeation studies with divalent cations show that the interactions between the ions and the charges of the selectivity filter domain are mainly of electrostatic nature. This result is remarkable when comparing it with the complexity of the selectivity for monovalent cations.

With a more negative net charge in the inner ring, the reversal potentials for Ba^{2+} currents (measured in whole cells) is increased (Fig. 5B; in Fig. 10B a pairwise comparison is shown). The channels are becoming increasingly more permeant to Ba^{2+} relative to the internal K^+ and Na^+ ions with more negative charges present.

Different binding strengths of divalent ions for three mutants with different charges in the filter region were observed before (Heinemann et al. 1992a). The results with the mutants investigated in the present study fit very well into this scheme (Fig. 8). After plotting the half-maximal concentrations for Ca_o^{2+} block as a function of the change in charge (Fig. 10C, pairwise comparison as in Fig. 10A),

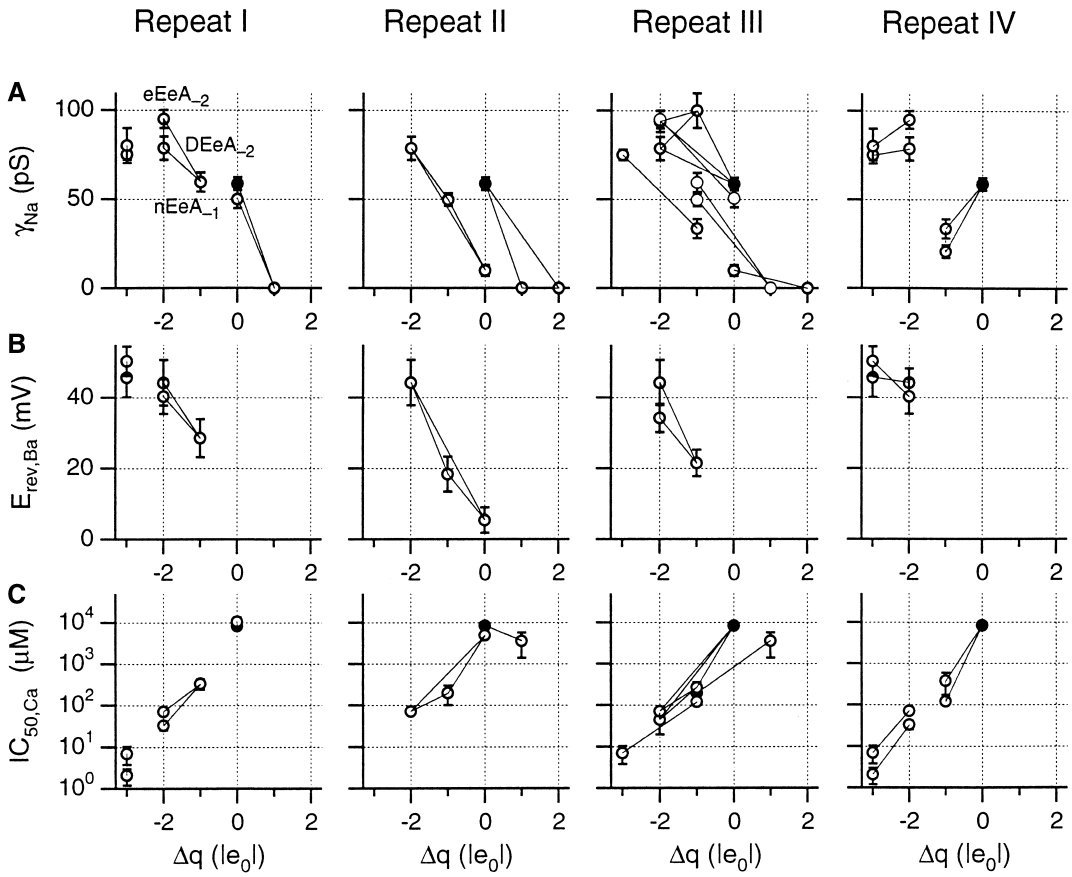

Fig. 10 Effect of single mutations on **A** the single-channel conductance (see also Table 1), **B** the reversal potential for Ba_o^{2+} (see also Fig. 5B), and **C** the Ca^{2+} block of sodium inward current (see also Table 2) for the inner ring positions of the four homologous repeats. In all three sections the value of the corresponding measured parameter is plotted versus the net change in charge of the inner ring relative to the wild type. The data points are always plotted as pairs of mutants, connected by a straight line, which only differ in a single position in the respective repeat, i.e. a line corresponds to a mutation. An example is given for two pairs of mutants in repeat I. With this presentation the effect of charge-changing and charge-conserving mutations can be visualized. While charge alterations in all four repeats have similar effects on Ca_o^{2+} block (**C**), this general tendency is not valid for repeat IV in respect to the single-channel conductance (**A**) and the whole-cell reversal potential measured in 75 mM extracellular Ba^{2+} (**B**). The filled circles in **A** and **C** denote the wild type. In part **A** the mutant $nEKA_{+1}$, which was reported to have a very small single-channel conductance (Pusch et al. 1991), was also included

the same tendency is found for all four positions in the different domains. With a more negative net charge in the inner ring, a lower $[Ca^{2+}]_o$ is needed to block the channel half-maximally.

Channel block by Ca_o^{2+} is strongly voltage dependent (Fig. 9). Therefore, in particular for mutants with a more negative inner ring structure than the wild type, the single-channel conductance can only be reliably estimated in Ca^{2+}-free solutions.

Unlike the channel block by divalent cations, the channel sensitivity towards TTX does not correlate strictly with the charge in the inner ring. This is not unexpected, because the major determinants for TTX binding to the channel are apparently located more towards the extracellular side of the channel like the putative outer ring and neighboring residues (Terlau et al. 1991; Backx et al. 1992; Heinemann et al. 1992b; Satin et al. 1992).

Parallels between Na- and Ca-channels

Studies with Ca-channels can be performed more systematically because of the presence of four glutamates in the inner ring structure. Several groups studied monovalent and divalent permeation in Ca-channel mutants in a similar way as we did in this study with Na-channel mutants (Yang et al. 1993; Tang et al. 1993; Heinemann et al. 1994; Ellinor et al. 1995; Parent and Gopalakrishan 1995). Measurements of the shift in reversal potential with high $[Ba^{2+}]_o$ in whole oocytes have revealed that the four positions do not contribute equally to ion selection; as in the Na-channel, mutation of the glutamate in the third domain results in a greater loss of selectivity of Ba^{2+} versus the internal cations than mutation of the equivalent glutamate in domain IV (Kim et al. 1993; Yang et al. 1993; Mikala et al. 1993; Heinemann et al. 1994). In the same studies it was found that substitution of the glutamates in the first two domains also affect the reversal potential to a degree which is similar to the effect of mutation of the glutamate in domain III.

Another parallel between Na- and Ca-channels is represented by the surprising finding that in the Ca-channel mutant EkEE (in the absence of divalent ions) the channel is more selective for bath-applied Na^+ (Mikala et al. 1993) and even more to Li^+ (Yang et al. 1993) in comparison to the internal ions, i.e. mainly K^+, while no comparable effects were found in Ca-channel single-site mutants with a lysine at one of the other three positions. The Ca-channel mutant EkEE may be compared to the Na-channel mutant $DkeA_0$ which also exhibits the permeability sequence $Li^+ > Na^+ > K^+$ (Table 1). This finding supports the notion that residues at equivalent positions in the two channel types determine similar channel properties. However, in the Ca-channel mutant EEka no enhanced selectivity of Na^+ over K^+ was found (Tang et al. 1993) indicating that it is not possible to confer Na-channel characteristics on the Ca-channel in a straightforward way.

In mutants of both channel types the Ba^{2+} reversal potentials as measured in whole cells are decreased with a more positive net charge of the inner ring (Fig. 5B for Na-channel mutants; Mikala et al. (1993) for Ca-channel mutants). This apparent resemblance is further supported by the fact that in both channel types this effect is much smaller for mutations in domain IV compared to the other domains. This presumably can be explained by the results of Chiamvimonvat et al. (1996b) and Pérez-García et al. (1996) who showed that the residue A1714 is located deeper in the channel pore than the other residues of the putative inner ring.

Not only the Ba^{2+} reversal potentials are affected to a similar extent by mutations in both channel types but also the ratio of maximum inward currents I_{Ba}/I_{Na}. In the Na-channel mutant $eEee_{-3}$ (Fig. 5A) as well as in the wild-type Ca-channel (Mikala et al. 1993) the maximum Ba^{2+} inward current is greater than the maximum Na^+ inward current. Similarly, the Ba^{2+} currents are smaller than the Na^+ currents in the Na-channel mutant $DkeA_0$ (Fig. 5A) and the Ca-channel mutant EkEE (Mikala et al. 1993). Furthermore, almost no Ba^{2+} currents could be measured through the Na-channel mutant $DEKe_{-1}$ and the Ca-channel mutant EEkE, whereas in both mutants the Na^+ currents are clearly measurable. In summary, in both channel types the permeation of Ba^{2+} is governed to similar extents by equivalent positions.

L-type Ca-channels exhibit permeation of Ca^{2+}, Sr^{2+}, and Ba^{2+} (e.g. Hess et al. 1986). Those Na-channel mutants which clearly show Ca^{2+} permeation are also permeant for Sr^{2+} and Ba^{2+} (e.g., Fig. 6). As in many Ca-channels (e.g., Hille 1992), Mg^{2+} and Mn^{2+} did not permeate detectably through the Na-channel mutants $DEee_{-3}$ and $eEee_{-3}$, i.e. those mutants which closely resemble Ca-channels in terms of the inner ring structure. Interestingly, Na-channel mutants with $\Delta q=-2$ and even $DEqA_{-1}$ are permeable for Mg^{2+} and Mn^{2+}. It remains unknown whether Mg^{2+} and Mn^{2+} permeation is prevented in the mutants $DEee_{-3}$ and $eEee_{-3}$ by the negative net charge (e.g. due to a strong binding of these ions in the channel) or if other steric constraints play a role as permeation only could be detected with an alanine residue in repeat IV.

As for the Na-channel mutants (Table 2, Fig. 8), the half-maximal Ca^{2+} block concentrations as a function of net charge in the inner ring structure were also determined for Ca-channel mutants (Ellinor et al. 1995). A comparison of the results from the two channel types shows parallels in this respect, too. The detailed studies with substitution of the glutamates with charged, polar and unpolar residues in the Ca-channel also revealed that polarity of the side chains is involved in binding of Ca^{2+} ions (Ellinor et al. 1995; Parent and Gopalakrishan 1995). Overall it can be stated that the IC_{50}'s for Ca^{2+} block are of the same order of magnitude for mutants of both channel types if they have equal net charge in the inner ring structures. This is especially remarkable for the IC_{50}'s of the Na-channel mutants $DEee_{-3}$ and $eEee_{-3}$ which have values in the range of μM (Table 2); the same is true for native Ca-channels (Kim et al. 1993; Tang et al. 1993; Yang et al. 1993; Mikala et al. 1993; Heinemann et al. 1994; Ellinor et al. 1995). Less agreement is obtained with respect to the Cd^{2+} block of Ba^{2+} currents which deviate by about one order of magnitude between the BI Ca-channel and the Na-channel mutant $eEee_{-3}$. Nevertheless, because of the low homology of the adjacent amino-acid residues in the two channel types it seems not very likely that other structural components participate strongly in the coordination of divalent cations.

Predictions for non-expressing putative Na-channel isoforms

While several Na-channel isoforms which could be expressed functionally in host cells share the common motif of the inner ring structure "DEKA" (e.g., brain: Noda et al. 1986; heart: Rogart et al. 1989; skeletal muscle: Trimmer et al. 1989), other isoforms which could not yet be expressed functionally were classified as Na-channels by means of sequence homology. Alignments of the pore regions of all four repeats of such isoforms reveal that their putative inner ring structures deviate strongly from the Na-channels expressed thus far. The Na-channel cloned from jelly fish (Anderson et al. 1993) has the motif $DkeA_0$. The corresponding mutant in NaRbII, however, resulted in channels with a significantly reduced selectivity for K^+ over Na^+ in addition to a measurable Ba^{2+} influx. More striking are the differences of the glial Na-channel with the inner ring motif $DEns_{-1}$ (Gautron et al. 1992, and personal communication Dr. Berwald-Netter), the Na-channel from squid: $DEet_{-2}$ (Sato and Matsumoto 1992), and from Drosophila: $DEeA_{-2}$ (Salkoff et al. 1987). Also deviating from the "typical" Na-channels is the motif $DEnA_{-1}$ of $hNa_v2.1$ from human heart and uterus which is a member of the Na-channel gene family 2 (George et al. 1992). Provided that one can transfer the results obtained from the mutagenesis of NaRbII to these channel isoforms, one would have to predict that all of these channels are relatively nonselective among monovalent cations; the latter two would even be predicted to be Ca^{2+} permeable. Therefore, it can be speculated that some of these channels have properties of both Na- and Ca- channels. For example, Ca^{2+} currents

sensitive to TTX, as found recently in human atrial cells (Lemaire et al. 1995), could be generated by such channels.

Acknowledgements We would like to thank A. Grimm and A. Roßner for technical assistance and Drs. W. Stühmer and H. Terlau for many discussions of this project.

References

Anderson PAV, Holman MA, Greenberg RM (1993) Deduced amino acid sequence of a putative sodium channel from the scyphozoan jellyfish *Cyanea capillata*. Proc Natl Acad Sci USA 90:7419–7423

Arellano RO, Woodward RM, Miledi R (1995) A monovalent cationic conductance that is blocked by extracellular divalent cations in *Xenopus* oocytes. J Physiol 484:593–604

Backx PH, Yue DT, Lawrence JH, Marban E, Tomaselli GF (1992) Molecular localization of an ion-binding site within the pore of mammalian sodium channels. Science 257:248–251

Barry PH, Lynch JW (1991) Liquid junction potential and small cell effects in patch-clamp analysis. J Membr Biol 121:101–117

Bénitah J-H, Tomaselli GF, Marban E (1996) Adjacent pore-lining residues within sodium channels identified by paired cysteine mutagenesis. Proc Natl Acad Sci USA 93:7392–7396

Bloomquist JR (1996) Ion channels as targets for insecticides. Annu Rev Entomol 41:163–190

Catterall WA (1988) Structure and function of voltage-sensitive ion channels. Science 242:50–61

Chiamvimonvat N, Pérez-García MT, Ranjan R, Marban E, Tomaselli GF (1996a) Depth asymmetries of the pore-lining segments of the Na^+ channel revealed by cysteine mutagenesis. Neuron 16:1037–1047

Chiamvimonvat N, Pérez-García MT, Tomaselli GF, Marban E (1996b) Control of ion flux and selectivity by negatively charged residues in the outer mouth of rat sodium channels. J Physiol 491:51–59

Chinn K, Narahashi T (1986) Stabilization of sodium channel states by deltamethrin in mouse neuroblastoma cells. J Physiol 380: 191–207

Ellinor PT, Yang J, Sathner WA, Zhang J-F, Tsien RW (1995) Ca^{2+} channel selectivity at a single locus for high-affinity Ca^{2+} interactions. Neuron 15:1121–1132

Favre I, Modczydlowski E, Schild L (1996) Structural determinants for K^+ and Ca^{2+} selectivity in the voltage-gated Na channel. Biophys J 40:A78

Gautron S, Dos Santos G, Pinto-Henrique D, Koulakoff A, Gros F, Berwald-Netter Y (1992) The glial voltage-gated sodium channel: cell- and tissue-specific mRNA expression. Proc Natl Acad Sci USA 89:7272–7276

George AL, Knittle TJ, Tamkun MM (1992) Molecular cloning of an atypical voltage-gated sodium channel expressed in human heart and uterus: evidence for a distinct gene family. Proc Natl Acad Sci USA 89:4893–4897

Heinemann SH, Schlief T, Mori Y, Imoto K (1994) Molecular pore structure of voltage-gated sodium and calcium channels. Brazilian J Med Biol Res 27:2781–2802

Heinemann SH, Stühmer W (1995) Molecular structure of potassium and sodium channels and their structure-function relationship. In: Sperelakis N (ed) Physiology and pathophysiology of the heart. Kluwer Academic Publishers, Boston, pp 101–114

Heinemann SH, Terlau H, Stühmer W, Imoto K, Numa S (1992a) Calcium channel characteristics conferred on the sodium channel by single mutations. Nature 356:441–443

Heinemann SH, Terlau H, Imoto K (1992b) Molecular basis for pharmacological differences between brain and heart sodium channel. Pflügers Arch 422:90–92

Hess P, Lansman JP, Tsien RW (1986) Calcium channel selectivity for divalent and monovalent cations. J Gen Physiol 88: 293–319

Hille B (1992) Ionic channels of exitable membranes. Sinauer Associates INC, Sunderland, Massachusetts

Kim MS, Morii T, Sun LX, Imoto K, Mori Y (1993) Structural determinants of ion selectivity in brain calcium channel. FEBS Lett 318:145–148

Kürz LL, Zuhlke RD, Zhang HJ, Joho RH (1995) Side-chain accessibilities in the pore of a K^+ channel probed by sulfhydryl-specific reagents after cysteine-scanning mutagenesis. Biophys J 68:900–905

Lemaire S, Piot C, Seguin J, Nargeot J, Richard S (1995) Tetrodotoxin-sensitive Ca^{2+} and Ba^{2+} currents in human atrial cells. Rec Channels 3:71–81

Leibowitz MD, Schwarz JR, Holan G, Hille B (1987) Electrophysiological comparison of insecticies and alkaloid agonists of Na channels. J Gen Physiol 90:75–93

Mikala G, Bahinski A, Yatani A, Tang S, Schwartz A (1993) Differential contribution by conserved glutamate residues to an ion-selectivity site in the L-type Ca^{2+} channel pore. FEBS Lett 335: 265–269

Neher E (1995) Voltage offsets in patch-clamp experiments. In: Sakmann B, Neher E (eds) Single-channel recording, 2nd edn. Plenum Press, New York, pp147–153

Noda M, Ikeda T, Kayano T, Suzuki H, Takeshima H, Kurasaki M, Takahashi H, Numa S (1986) Existence of distinct sodium channel messenger RNAs in rat brain. Nature 320:188–192

Noda M, Suzuki H, Numa S, Stühmer W (1989) A single point mutation confers tetrodotoxin and saxitoxin insensitivity on sodium channel II. FEBS Lett 259:213–216

Parent L, Gopalakrishan M (1995) Glutamate substitution in repeat IV alters divalent and monovalent cation permeation in the heart Ca^{2+} channel. Biophys. J. 69:1801–1813

Pérez-García MT, Chiamvimonvat N, Marban E, Tomaselli GF (1996) Structure of the sodium channel pore revealed by serial cysteine mutagenesis. Proc Natl Acad Sci USA 93:300–304

Pusch M, Noda M, Stühmer W, Numa S, Conti F (1991) Single point mutations of the sodium channel drastically reduce the pore permeability without preventing its gating. Eur Biophys J 20: 127–133

Rogart RB, Cribbs LL, Muglia LK, Kephart DD, Kaiser MW (1989) Molecular cloning of a putative tetrodotoxin-resistant rat heart Na^+ channel isoform. Proc Natl Acad Sci USA 86:8170–8174

Salkoff L, Butler A, Wei A, Scavarda N, Giffen K, Ifune C, Goodman R, Mandel G (1987) Genomic organization and deduced amino acid sequence of a putative sodium channel gene in *Drosophila*. Science 237:744–749

Satin J, Kyle JW, Chen M, Bell P, Cribbs LL, Fozzard HA, Rogart RB (1992) A mutant of TTX-resistant cardiac sodium channels with TTX-sensitive properties. Science 256:1202–1205

Sato C, Matsumoto G (1992) Primary structure of squid sodium channel deduced from the complementary DNA sequence. Biochem Biophys Res Com 186:61–68

Stühmer W, Conti F, Suzuki H, Wang X, Noda M, Yahagi N, Kubo H, Numa S (1989) Structural parts involved in activation and inactivation of the sodium channel. Nature 339:597–603

Stühmer W, Terlau H, Heinemann SH (1992) *Xenopus* oocytes for two electrode and patch clamp recording. In: Kettenmann H, Grantyn R (eds) Practical electrophysiological methods. Wiley-Liss, New York, pp121–125

Tang S, Mikala G, Bahinski A, Yatani A, Varadi G, Schwartz A (1993) Molecular localization of ion selectivity sites within the pore of a human L-type cardiac calcium channel. J Biol Chem 268: 13026–13029

Terlau H, Heinemann SH, Stühmer W, Pusch M, Conti F, Imoto K, Numa S (1991) Mapping the site of block by tetrodotoxin and saxitoxin of sodium channel II. FEBS Lett 293:93–96

Tomaselli GF, Chiamvimonvat N, Nuss HB, Balser RB, Pérez-García MT, Xu RH, Orias DW, Backx PH, Marban E (1995) A mutation in the pore of the sodium channel alters gating. Biophys J 68: 1814–1827

Trimmer JS, Cooperman SS, Tomiko SA, Zhou J, Crean SM, Boyle MB, Kallen RG, Sheng Z, Barchi RL, Sigworth FJ, Goodman RH, Agnew WS, Mandel G (1989) Primary structure and functional expression of a mammalian skeletal muscle sodium channel. Neuron 3:33–49

Tsushima R, Li R, Backx PH (1996) Altered ionic selctivity of the Na^+ channel revealed by cysteine mutations in the P-loop of domain IV. Biophys J 70:A24

West JW, Patton DE, Scheuer T, Wang Y, Goldin AL, Catterall WA (1992) A cluster of hydrophobic amino acid residues required for fast Na^+-channel inactivation. Proc Natl Acad Sci USA 89:10910–10914

Yang J, Ellinor PT, Sather WA, Zhang J-F, Tsien RW (1993) Molecular determinants of Ca^{2+} selectivity and ion permeation in L-type Ca^{2+} channels. Nature 366:158–161